Technical Document 2730
October 1994

Measurements of Ionospheric Variability

R. A. Sprague

CONTENTS

Figures

Table

INTRODUCTION

The earth's ionosphere has been studied extensively for the past 50 to 60 years. This interest has been partially driven by the ionosphere's ability to reflect radio waves transmitted from ground-based transmitters when the frequency of the waves lies in the high-frequency (HF) band (2 to 30 MHz). Since the dominant reflecting layer is some 100 to 700 km above the earth's surface, this ability makes communication to a receiver that lies beyond the line-of-sight (BLOS) of the transmitter possible. In the last 30 years, satellites have become the primary tool for such long-haul communications; however, HF is still used in many military applications, and it remains the only option for BLOS communication in some countries.

Continuous monitoring of the ionosphere at a group of ionospheric stations scattered around the world began in the 1940s, and the data collected have been used for development of radio propagation models. The models are used to select operational frequencies within the HF band for existing systems and to aid in the design of new systems.

Early on, it was assumed that ionospheric properties change rather slowly, being driven primarily by the daily transit of the sun and the even slower changing of the seasons. In that case, monthly median models of ionospheric parameters were assumed to be adequate in most applications. Most of the long-term measurement programs were designed to provide data suitable for input in the design of such models, and thus, a typical measurement schedule might include sampling the ionosphere at 15-minute or 1-hour rates.

However, within the past 10 to 15 years, the high level of ionospheric variability on time scales as short as 10 to 15 minutes has come to be recognized. This variability, driven primarily by local disturbances in the neutral atmosphere at mid-latitudes, has been found to be the rule rather than the exception in the ionosphere. It is this short-time-scale variability and its resultant effects on military systems that are the subject of this measurement effort.

Two separate measurement campaigns are being staged. In the first, measurements of the effect of the short-time-scale ionospheric variations on HF skywave signal power are being made to assess their impact on military communication systems. Data collected in this effort are used to verify the predictions of current median propagation models and to develop new models that incorporate the effects of the short-term variability.

In the second measurement effort, the Naval Command, Control and Ocean Surveillance Center (NCCOSC) RDT&E Division (NRaD) vertical incidence ionosonde is being used to collect data to directly determine the scale, in time, of ionospheric variability. A similar ionosonde, owned and operated in Utah by Utah State University, is also collecting data on a schedule compatible with the NRaD sounder. Comparison of simultaneous data collected at the two sites will be used to determine the spatial scale of the variability. This measurement effort is partially funded by the Independent Research program at NRaD. In this report, progress made in both efforts during FY 94 will be discussed.

SKYWAVE SIGNAL POWER MEASUREMENTS

Data for this effort are being collected on a 1750-km transmission path established between Montana and California. Continuous wave (CW) signals are transmitted from a site near Forsyth, MT, and received in Imperial Beach. CA, which is approximately 20 miles south of San Diego near the U.S. Mexico border. Details of the transmitter and receiver installations, a description of the transmission schedule, and examples of the raw data are given in earlier reports (Sprague, 1994 and Sprague, Moision, and Theisen, 1994).

A unique aspect of this measurement effort, aside from the short-time-scale resolution of the measurements, is the simultaneous determination of the propagating mode structure for each frequency and for each measurement. This is accomplished by the operation of an oblique ionospheric sounder in conjunction with the measurement system as described by Sprague, Moision, and Theisen, 1994. It was initially hoped that data downloaded from the sounder receiver by the controlling computer after each measurement period would be sufficient for mode determination. However, it has been determined that such data are not adequate for providing the detailed determination of all propagating modes that is required in this effort. Consequently, a second oblique sounder has been installed near the receiver site for the sole purpose of providing hardcopy printouts of each oblique ionogram obtained during a measurement period. Determination of modes is done manually by inspection of the hardcopy ionograms. This tedious process requires a trained analyst and has significantly increased the time required to fully analyze the data.

As discussed in Sprague, Moision, and Theisen, 1994, the choice of transmission paths was partially driven by the requirement that a vertical incidence ionosonde (VI) operating on a time schedule compatible with the measurement schedule be located near the midpoint of the path. The intention was to use ionograms obtained by the VI to define the ionosphere for each measurement period. A ray-tracing program would then be used to determine the take-off and reception angle for each propagating mode in order to assign antenna gains to each mode.

Significant effort was spent in preparing and testing a suitable raytrace program that would accept the parameter set scaled from the ionograms obtained from the VI. However, several problems were encountered that make the use of this technique impractical at this time. First, the program used to scale the ionograms taken at the VI site only obtains parameters for the ionospheric F-layer. During daylight hours, the F region usually consists of two separate layers, the F2- and Fl-layers. In this case, the program only scales the F2-layer parameters. However, for path lengths less than about 2000 km and especially for spring/summer periods in low sunspot years, the lower (in height) F1-layer often controls the propagation on the path. This has been verified in many of the oblique ionograms examined on this path. The consequences for this effort are that a model of the F1-layer must be used in the raytrace program to predict modal angles for the Fl-layer modes. However, the model is in many instances incompatible with the actual measured F2-layer data, thus producing an unrealistic modal prediction and, many times, falling to predict modes even when the modes are clearly present on the oblique ionograms.

A similar problem is the appearance of E-layer modes on the oblique ionograms. Since the VI scaling program produces only minimal information on E-layer parameters, it is often necessary to supplement that information with an E-layer model for use in the raytrace program. In those instances, problems similar to those described above for the Fl-layer are encountered.

Finally, the ionosphere at the path midpoint is quite often disturbed, especially in the evening hours. The disturbance manifests itself by the presence of spread-F on ionograms. During spread-F conditions, the ionospheric reflecting surface is often pictured as a corrugated surface, like the surface of a rough ocean. This corrugation produces multiple reflection points and a resultant spread in the virtual heights for a given frequency of a vertical ionogram. The presence of spread-F on ionograms makes it very difficult to scale the parameters required by the raytrace program.

Although means for working around some of these problems are being developed, at this point it makes little sense to invest the time and effort necessary to obtain highly accurate modal angles from the VI data. Thus, an analytical method using fixed reflection heights for each mode type will be used initially. A simple geometric analysis using the reflection heights shown in table I results in the modal angles for each frequency/mode combination shown in that table. Note that errors using this technique are unlikely to cause more than 2 or 3 dB errors in the estimated antenna gains for 1- and 2-hop

F-layer modes or I-hop E-layer modes because of the relatively large lobe-width in elevation angle for the 1/4-wavelength antennas used in this effort.

Table 1. Take-off and reception angles for modes assuming fixed heights.

Mode	Reflection Height (km)	Take-Off/Reception Angle (deg)
1-hop E (night/day)	100	2.4
1-hop F2 (day)	300	14.3
1-hop F (night)	450	22.1
1-hop F (transition)	375	18.4
1-hop F1 (day)	200	8.5
2-hop F2 (day)	300	31.5
2-hop F (night)	450	42.5
2-hop F (transition)	375	37.5
3-hop F2 (day)	300	43.5
3-hop F (night)	450	54.5
3-hop F (transition)	375	49.7

As described in Sprague, Moision, and Theisen, 1994, measurements are made for a total of 30 seconds on each frequency every 5 minutes. During the first 15 seconds, the transmitter in Montana is off, and the background noise level is measured. For the second 15 seconds, the 150-watt (5l.76-dBm) CW transmitter is on, and measurements of signal+noise are obtained. Data samples, in dBm (dB relative to I milliwatt), are obtained at 30-ms intervals in a l00-Hz bandwidth.

To obtain estimates of received signal power, it is necessary to subtract the noise from measurements of signal+noise. Thus, accurate measurements of noise are required. The receiver used in this measurement system is an HP spectrum analyzer that has a 26-dB noise figure. This yields an average noise level of –l28 dBm in the 100-Hz bandwidth. To improve the system performance, a 19-dB preamplifier with a 5-dB noise figure has been installed before the spectrum analyzer. The cascaded system noise figure is then about 10 dB, resulting in an average noise level of about –144 dBm in a 100-Hz bandwidth (Kandoian, 1968). This level is well below the measured noise levels and so should not contribute significantly to our measured data.

Figure 1 shows monthly median noise measurements at 3.35 MHz for April (top) and May (bottom) 1994. In this figure and in the other figures shown here, monthly median values are obtained from the measurements by first estimating the median value for each individual measurement period. Thus, data collected during each 15-second measurement period are sorted, and the median and 10th and 90th percentile values of the data are determined. This results in 12 median values (every 5 minutes) for each hour of each day within a month. The median values for each hour for all the days of the month are then combined, sorted, and the median and decile values are determined for each hour. We thus obtain monthly median, and 10th, and 90th percentile values for each hour and for each frequency for the month.

Figure 1 shows that the Imperial Beach receive site is a very high-noise location at 3.35 MHz throughout the day. Curves A through E in the figure are the International Radio Consultative Committee (CCIR) model estimates for median noise level at 3.35 MHz for the Imperial Beach site. Curves A through D correspond to man-made noise estimates for “business,” “residential,” “rural,”

and “quiet rural” sites, respectively (CCIR, 1990). Curve E represents model estimates of median atmospheric noise power at the site. The figure shows that, for both months, the measured median noise level is approximated quite well by the “business” man-made noise type for most hours of the day. This agrees well with previous estimates of the noise level at this site (Sailors, 1990). However, for both months, there is a relatively slow rise in the median noise level beginning near local midnight that is maintained for 5 to 6 hours until sunrise. The source of this increase in the noise level is unknown at this time.

Figure 2 shows the measured signal power at 3.35 MHz for April (top) and May (bottom) 1994. Data for this figure were obtained by subtracting measured noise power from measured values of signal+noise. The data have been corrected for system losses (Sprague, Moision, and Theisen, 1994), but antenna gains have not been subtracted. For each month, peak nighttime median signal powers of about –60 dBm are obtained, while the daytime values drop to around –90 dBm, the noise level shown in figure 1. This is, of course, the expected diurnal behavior for the 3.35-MHz signal.

Also indicated in figure 2 are the 10th and 90th percentile values of the median distribution for each hour. The data for April indicate skewed hourly distributions of the median signal power with a large tail toward lower signal levels. The May data show relatively symmetric hourly distributions with much smaller spread. The hourly distributions are wider at night, when signals are propagating, than during the day.

In figure 3, the measured hourly median signal-to-noise (S/N) ratios for April (top) and May (bottom) at 3.35 MHz are compared to PROPHET predictions. PROPHET is a propagation prediction program developed and maintained by NRaD. PROPHET uses a largely empirically derived method for predicting signal strengths (Sailors and Rose, 1993). The CCIR man-made noise models and an atmospheric noise model by Sailors (Sailors and Brown, 1983) are used for prediction of S/N. No attempt to assess the accuracy of PROPHET in determining the actual propagating mode structure has been made for this figure. In general, PROPHET only determines one F-layer mode, one E-layer mode, and possibly, one mixed mode (Sailors and Rose, 1993). At any given hour, the actual propagation modal structure may differ significantly from that determined by PROPHET. Thus, more (or less) modes may actually be present in the measured data. This affects the total received power and will contribute to errors in prediction.

In the top plot of figure 3, April 1994 data are shown. In this plot, “quiet rural” man-made noise type is used in model predictions, which should significantly underestimate the noise environment as determined in figure 1. As seen in the top plot of figure 3, the model S/N does exceed the measured data for most hours, except in the late evening hours when predictions agree well with the data. Since there is no diurnal dependence in the man-made noise model, using the “business” noise type may produce better predictions over most of the day, at the expense of a large error in the late evening hours.

The bottom plot in figure 3 shows a corresponding comparison between PROPHET and measured data for May 1994. In this case, the appropriate “business” noise type was used in PROPHET predictions. Predictions in this case are quite good, with less than 10-dB error during the evening hours.

Figure 4 shows the measured monthly median noise levels at 7.8 MHz for April (top) and May (bottom) 1994. The April data show that, for this month, nighttime noise levels are best approximated by the “business” man-made noise type. However, unlike the noise at 3.35 MHz, the noise at 7.8 MHz shows a diurnal trend with levels dropping 8 to 10 dBm during the day. The diurnal trend closely follows model predictions for atmospheric noise, but the levels exceed atmospheric noise by 6 to 10 dBm during the night and 20 to 25 dBm during the day.

In contrast, the May data shown in the bottom plot of figure 4 show extremely high noise levels for all hours. Nighttime levels exceed “business” man-made noise type by 25 dBm and atmospheric levels by 30 dBm. Daytime noise levels drop to within 2 to 3 dBm of “business” type. Again, a strong diurnal trend that closely matches the atmospheric noise trend is visible.

Figure 5 shows monthly median measured signal power at 7.8 MHz for April (top) and May (bottom) 1994. Data for April show a relatively flat diurnal curve with a difference of no more than 25 dBm between day and night. The plot shows that the hourly distributions for April are skewed toward lower values during the day and toward higher values at night.

May data shown in the bottom plot of figure 5 show an almost linear decrease in median signal power from early evening to midday, with very little discernible diurnal trend. Hourly distributions are relatively narrow and symmetric during most of the day, with a large spread during several hours after local midnight. During this period, the distribution is strongly skewed toward lower signal levels.

Figure 6 compares the monthly median measurements of S/N at 7.8 MHz for April (top) and May (bottom) 1994 with PROPHET predictions. For the April data, a “quiet rural” man-made noise type was assumed, which greatly underestimates the true noise environment as shown in figure 4. This underestimate of the noise power is immediately evident in the 35 -dBm overprediction of S/N during the nighttime hours. However, a relatively strong diurnal trend is visible in the measured data while the model predictions are virtually flat during the same period. Since the man-made noise has no diurnal trend, a more complicated model would be required to adequately model the nighttime behavior of S/N.

For the May data of figure 6, a “business” man-made noise type was assumed, and the predictions still are overly optimistic during the nighttime noise. This is due to the extremely high nighttime noise levels measured during May at 7.8 MHz as shown in figure 4. Daytime predictions using “business” noise type provide fairly accurate predictions.

Figure 7 shows the monthly median noise power measured at 14.4 MHz in April (top) and May (bottom) 1994. The April noise data are best approximated by the “rural” man-made noise type during most of the day. In the post-noon hours, the atmospheric noise model exceeds the “rural” man-made noise type, and the measured data show a similar behavior. Data for May show a similar behavior at all hours although, in the early evening hours, noise levels are 4 to 5 dBm larger than the April data.

The measured signal power at 14.4 MHz for April (top) and May (bottom) 1994 is shown in figure 8. The April median signal power shows a strong diurnal trend, with daytime levels some 30 dBm larger than the nighttime levels. This is to be expected for the 14.4-MHz signal. The hourly median distribution spread is large at night, when it essentially corresponds to the spread of the local noise distribution. At these times, the distributions are skewed with large tail extending toward larger values. During daylight hours, the hourly distribution spread is also large, with the distribution strongly skewed toward weaker signals. The abrupt increase in median signal power at sunrise is clearly evident.

The May signal power data are shown in the bottom plot of figure 8. The median data again show a strong diurnal trend with a rapid rise at sunrise. However, unlike the April data, an abrupt reduction in signal power is also evident in the early evening hours, corresponding to sunset. The hourly distributions are mostly symmetric around the median level, and the spread of the distributions is smaller than that seen in the April data.

Finally, figure 9 shows a comparison of measured median S/N and PROPHET predictions for the 14.4-MHz signal for April (top) and May (bottom) 1994. Again, the April predictions were made

assuming a “quiet rural” man-made noise type, which, for this frequency, is closer to the measured noise levels. The predictions for April are quite good in the post-sunrise hours, with a fairly strong overshoot at sunrise. However, the late afternoon and early evening predictions are optimistic by some 35 dB. This is clearly due to the lack of a strong signal at these hours, which is evident in figure 8.

The May S/N data shown in the bottom plot of figure 9 are in good agreement with model predictions, assuming “business” man-made noise type, throughout the day. In particular, the strong signal level in the late afternoon and early evening hours for May causes the measured S/N to be in good agreement with the model during these hours.

The results presented in the previous figures are intended to indicate the type of analysis that is being done on the measured data. In these examples, monthly median data have been extracted for the purpose of comparison and validation of a model that predicts such parameters. Information regarding the day-to-day and within-the-hour variability of signal and noise power is also being extracted for verification of models that use such information for prediction of the reliability of the median predictions.

Particularly evident in the results presented here and in the data examined to date is the fact that the Imperial Beach location is an extremely high noise site. While the site is somewhat removed from major industrial facilities, its location is very near the ocean and San Diego Bay, which separates it from a large industrial region near downtown San Diego. The use of vertical antennas for reception makes the system particularly susceptible to ground-wave noise, which propagates with little attenuation over the ocean surface, even at 14.4 MHz. This may contribute to the strong noise levels evident in the data, at all frequencies, throughout the day and night.

VERTICAL SOUNDING MEASUREMENTS

A second measurement campaign is also being undertaken to directly detect ionospheric variability. This effort uses the vertical incidence sounder at the NRaD site in San Diego to determine the temporal scales of F2-region variability and the hours of the day when ionospheric variability is most prevalent. A second sounder located near Bear Lake, Utah, and operated for this project under contract to NRaD by Utah State University, is also collecting data on a synchronous schedule with the San Diego sounder. Future plans are to search for any spatial correlations in variability at the two sites. Work for this effort is partially funded by the Independent Research program at NRaD.

In order to characterize the temporal dependence of the F-region ionosphere, a “variability index” has been developed. The method used to obtain the index is somewhat different than the method envisioned earlier (Sprague, 1994; Sprague and Paul, 1993). The original method attempted to take advantage of the natural separation of F-region variability time scales into periods greater than about 3 hours and those less than 3 hours. The variations with periods less than 3 hours are of interest in this effort since they are largely driven, at mid-latitudes, by variations in the neutral atmosphere and are omnipresent in ionospheric data. Variations with periods greater than about 3 hours are driven mainly by large-scale processes associated with daily and seasonal changes in the solar zenith angle. These longer period variations are well understood and, for the most part, easily predictable.

In the earlier method, the daily measured data were filtered to remove variations longer than 3 hours. The filtered data were then subtracted from the original data to obtain data with periods shorter than 3 hours removed. The root-mean-square (RMS) of this short period data was then to be used as the variability index. However, the measured data are often plagued with noise that produces spurious or missing data points that must be filled in by interpolation. This produces “outlying” data

points that completely control the RMS values for the day, so a true estimate of the RMS values cannot be obtained. For these reasons, a second method has been employed to establish the variability index.

The second method calculates the time rate of change between two consecutive data points (data are taken at 5-minute intervals), so no distinction is made between predictable diurnal and unpredictable short-time-scale random variations. This approach may be more useful in practice since an estimate of the total variability of a parameter is required, and the cause of the variability is of little importance.

The determination of the variability index proceeds in several stages. First, the selected parameter is extracted from the daily records of ionospheric data and examined visually for noisy data. Outliers are linearly interpolated into the average trace. This step has been found to be necessary for only about 1 percent of the San Diego data.

With the basic data set prepared, the absolute value of the time rate of change over the 5-minute time increment is calculated for all days of the month for which data are available. Only data for which consecutive data points are available are considered; if data are missing, the data points are ignored. Each rate of change value is then multiplied by 12 to provide an estimate of the equivalent rate of change over an hour. When a complete month of data is obtained, median and selected percentile values are determined for each hour.

Figure 10 shows the hourly median values of the time rate of change of the MUF(3000) for the winter months January (top), February (middle), and March (bottom) 1994. Data shown in this figure and in figures 11 through 14 have been further smoothed by calculating a seven-point running average of consecutive data points (35 minutes) in order to emphasize major trends. Clearly visible in all 3 months is the expected increase in variability during sunrise and sunset periods. More interesting is the almost linear reduction of variability from the post-sunrise period. This trend continues, interrupted only by the peak near sunset, during the daylight hours. Nighttime values are approximately constant for the MUF(3000). Very similar behavior is seen in the 1993 data for the same 3 months.

Figure 11 shows the hourly median values of the time rate of change of the MUF(3000) for May (top), June (middle), and July (bottom) 1993. In contrast to the results shown in figure 3, results for May, June, and July show little diurnal change in the variability. There is an indication of a rise in variability at sunrise, but the levels are maintained throughout the entire day. There is no indication of a sunset peak in the May, June, and July data.

Variability for the F-region critical frequency, foF2, is shown in figure 12 for winter months January (top), February (middle), and March (bottom) 1993. Here again, there is a strong peak at sunrise and an approximately linear reduction throughout the day, broken by a secondary peak at sunset. Like the results for the MUF(3000) shown in figure 10, nighttime variability remains approximately constant for the foF2.

Variability data for the F-region density height, hmF2, are shown in figure 13 for November (top) and December (middle) 1992 and January (bottom) 1993. Characteristics of the variability for hmF2 is quite different from that for MUF(3000) and foF2, with large variations present throughout the nighttime hours and relatively low levels during daylight hours. This behavior for the hmF2 is consistent with earlier results concerning this parameter (Paul, Sprague, and Moision, 1992).

Finally, variability data for the half-thickness, ymF2, of the F-region for November (top) and December (middle) 1992 and January (bottom) 1993 are shown in figure 14. Variability of ymF2 is similar to that shown in figure 13 for the layer peak height, with high levels at night and relatively low levels throughout the daylight hours.

The variability indices shown in figures 10 through 14 were all obtained from San Diego data. As mentioned above, the Utah site is also collecting data on a schedule compatible with San Diego, and the intention is to compare the indices derived in San Diego with similar indices obtained from the Utah data. However, the Utah data consist of raw ionograms that must be scaled to generate the parameters necessary to derive the vulnerability indices. Efforts to scale the Utah data are continuing, but there is considerable effort required to obtain reliable parameters from the Utah data, which are much noisier than the San Diego data. Noisy data cause problems for O–X mode determination, which is critical for accurate ionogram scaling. Also, the ionosphere is considerably more variable at the higher latitude Utah site, with a high incidence of nighttime spread-F that makes the ionograms very difficult or impossible to scale.

During this fiscal year, an improved scaling method that appears to be capable of scaling ionograms during light spread-F conditions has been developed by Paul (1994, private communication). Work is currently underway to rescale both the Utah and San Diego data using the new program in the hope that more usable data can be obtained for both sites.

DISCUSSION

Current plans call for continued data collection for FY 95. Some of the signal power data collected during FY 94 remain to be prepared for comparison to model predictions. Also, mode determination for the FY 94 data will require considerable effort. The comparison of actual propagating modes to those predicted by a model program is an important factor in assessing the accuracy of predicted signal power. The mode determination is also of interest for its own sake since it is another way to verify the accuracy of ionospheric and propagation models.

A possibly important feature in determining the level of ionospheric variability is the activity level of the sun. We are currently in the period of solar sunspot minimum, and the sun is generally much less active than during the sunspot peak period. Thus, it is important that vertical ionosonde data continue to be collected so that the effects of the increased solar activity on the variability index can be determined.

REFERENCES

International Radio Consultative Committee (CCIR) XVIIIth Plenary Assembly, Dusseldorf. 1990. "Man-Made Radio Noise; Report 258-5," *Propagation in Ionized Media, Recommendations and Reports of the CCIR,* vol. VI, Geneva, Int. Telecommun. Union.

Kandoian, A. G. 1968. *Reference Data for Radio Engineers,* Fifth edition, A. G. Kandoian, ed., Howard W. Sams & Co., Inc.

Paul, A. K., R. A. Sprague, and W. K. Moision. 1992. "Comparison of San Diego Observations [March 1992] with International Reference Ionosphere Predictions," in *Data Validation of Ionospheric Models and Maps,* Publicaciones del Observatorio del Ebro, *Memoria* 16, Roquetes (Tarragona) Spain.

Sailors, D. B. 1990. "Techniques for Estimating the Effects of Man-Made Radio Noise on Distributed Military Systems," *NATO Agard Conference Proceedings 486,* papers presented at the Electromagnetic Wave Propagation Panel Symposium, Rethymno, Crete, Greece, 15–18 Oct.

Sailors, D. B. and R. P. Brown. 1983. "Development of a Minicomputer Atmospheric Noise Model," *Radio Sci.,* vol. 18, pp. 625–637.

Sailors, D. B. and R. B. Rose. 1993. “HF Sky-wave Field Strength Predictions,” NRaD TR 1624 (Sept). Naval Command, Control and Ocean Surveillance Center, RDT&E Division, San Diego, CA.

Sprague, R. A. 1994. “Atmospheric Effects Assessment Program: Ionospheric Sounding,” NRaD TD 2609 (Feb). Naval Command, Control and Ocean Surveillance Center, RDT&E Division, San Diego, CA.

Sprague, R., W. Moision, and J. Theisen. 1994. “High-Frequency Skywave Signal Power Measurement System,” NRaD TD 2664 (July). Naval Command, Control and Ocean Surveillance Center, RDT&E Division, San Diego, CA.

Sprague, R. A. and A. K. Paul. 1993. “High Time Resolution Measurements of Ionospheric Variability,” paper presented at the 1993 Ionospheric Effects Symposium, Alexandria, VA, 4–6 May.

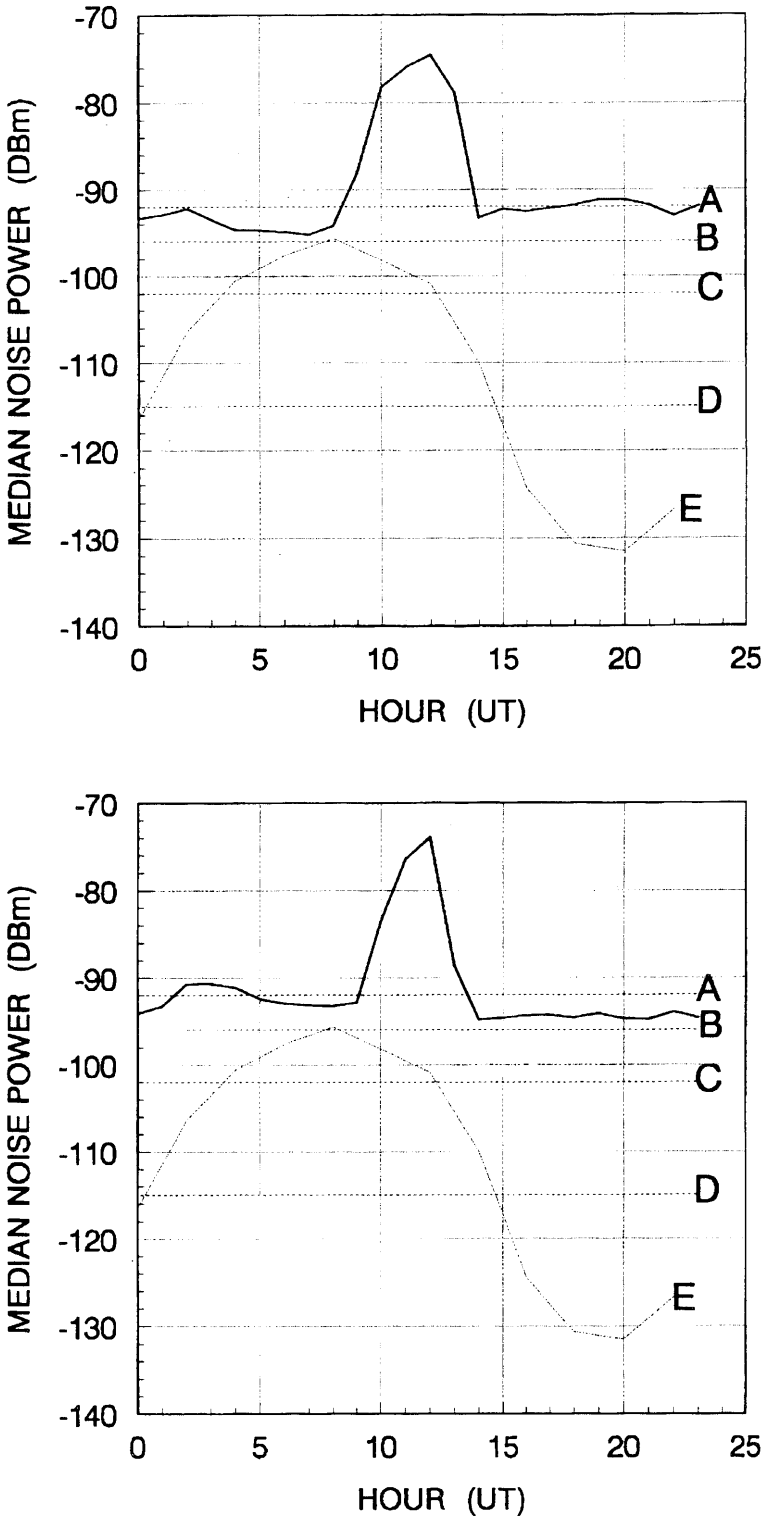

95088001/1

Figure 1. Median noise at 3.35 MHz for April (top) and May (bottom) 1994. Curves A through D are man-made noise estimates for business, residential, rural, and quiet rural, respectively. Curve E is the estimated atmospheric noise level for the Imperial Beach site.

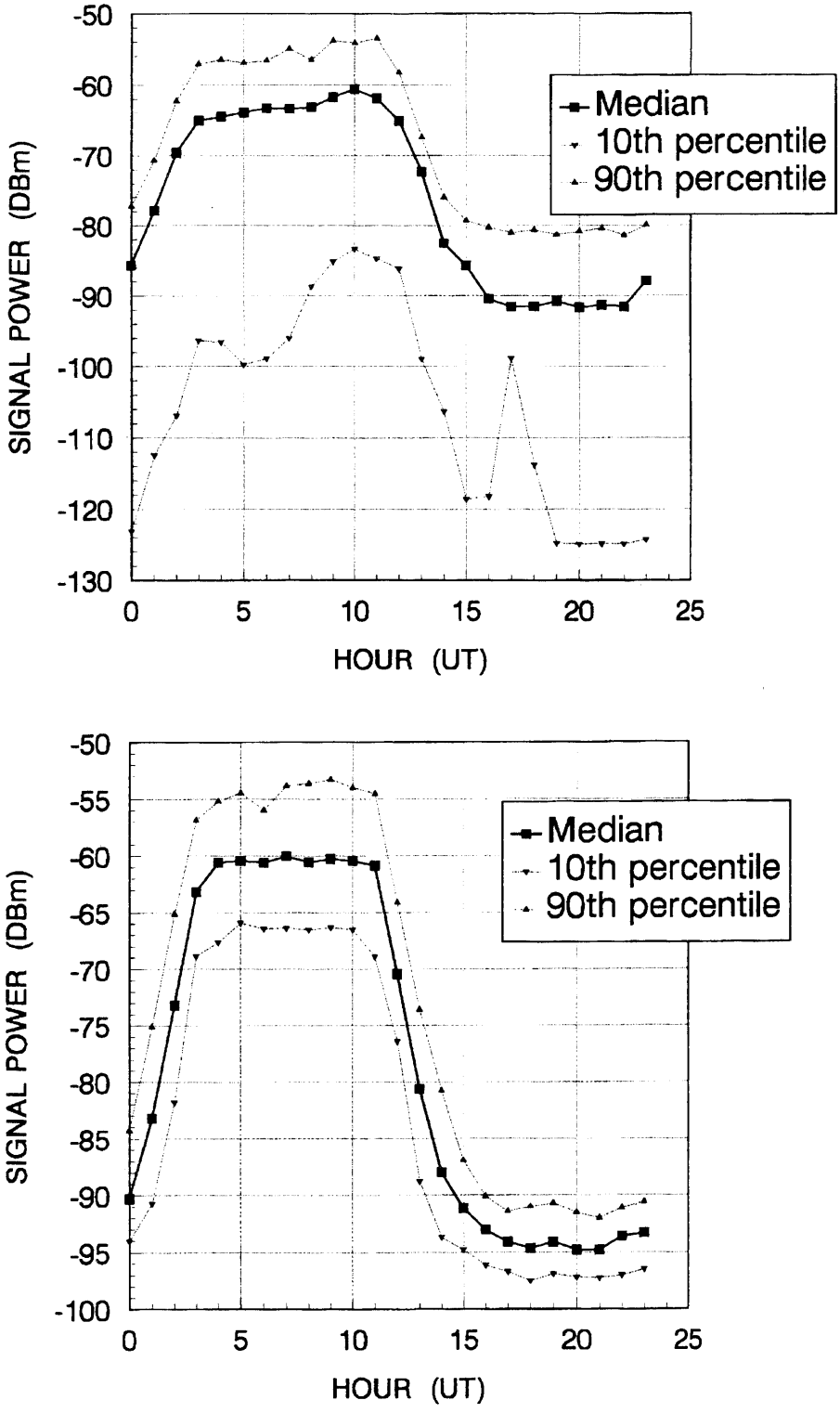

95088002/1

Figure 2. Signal power at 3.35 MHz for April (top) and May (bottom) 1994. Median, 10th percentile, and 90th percentile of the hourly monthly median distribution are shown in separate curves.

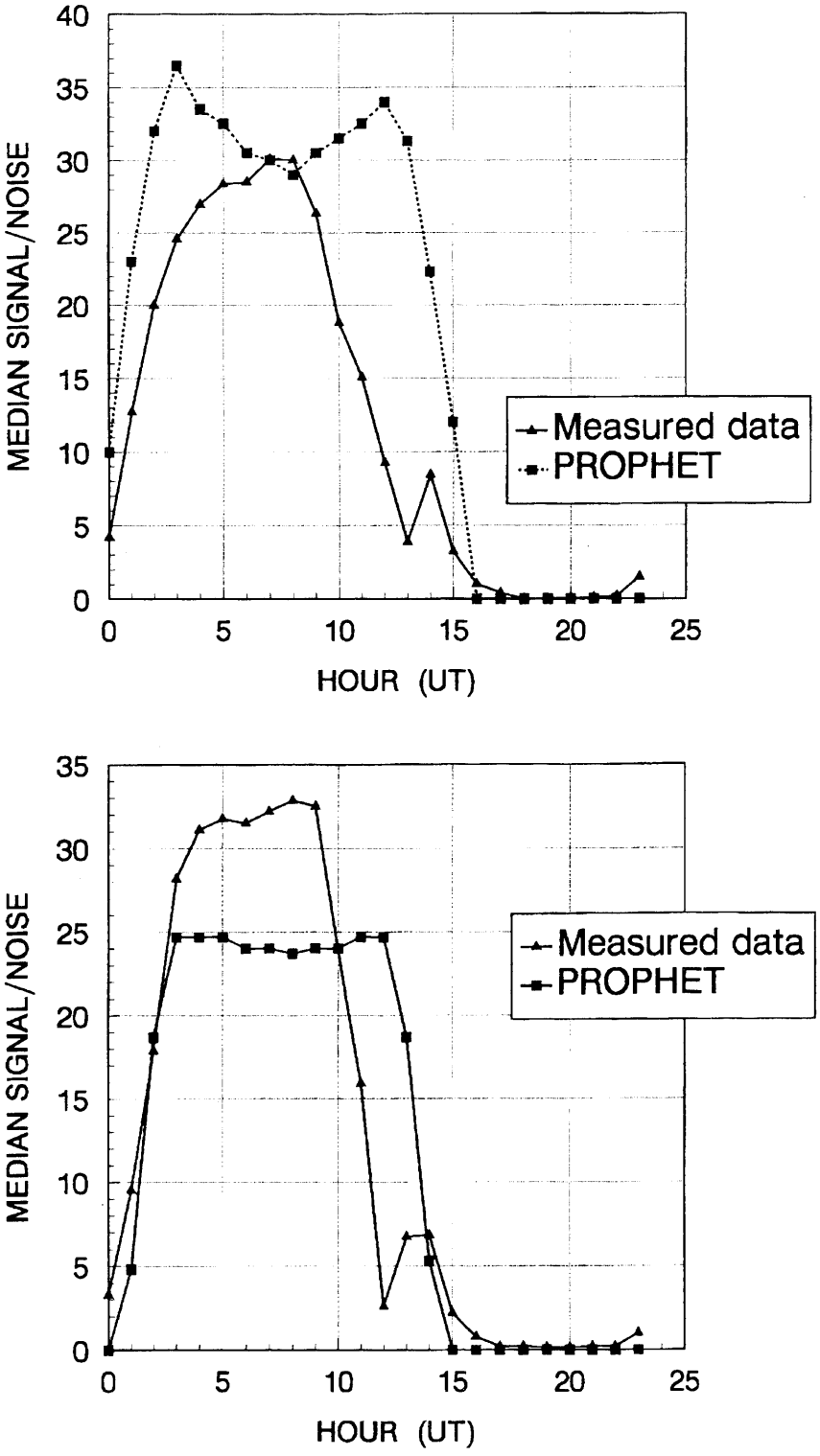

95088003/1

Figure 3. Median signal-to-noise ratio at 3.35 MHz for April (top) and May (bottom) 1994. Also shown are PROPHET predictions for the same period.

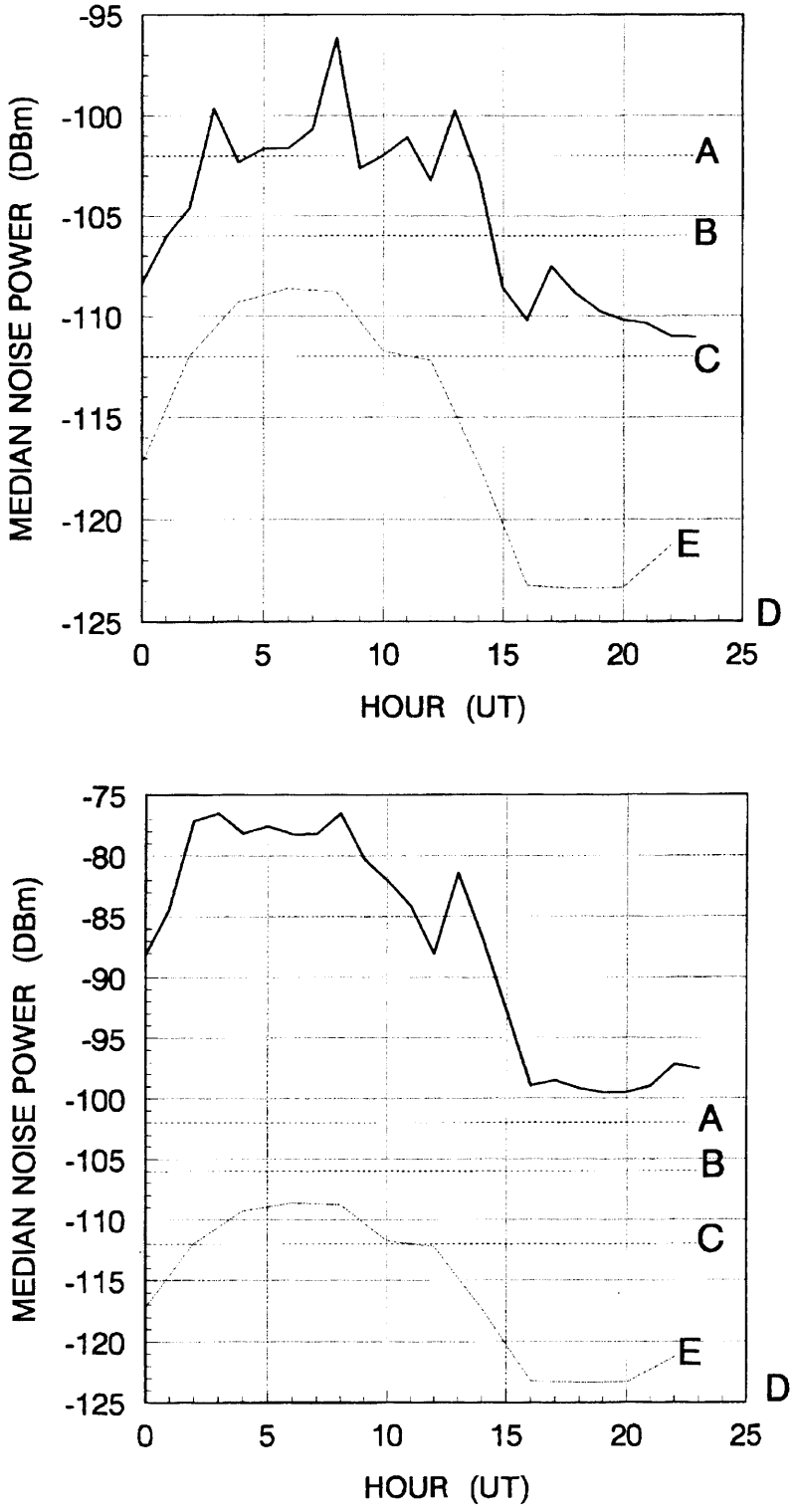

95088004/1

Figure 4. Median noise at 7.8 MHz for April (top) and May (bottom) 1994. Curves A through D are man-made noise estimates for business, residential, rural, and quiet rural, respectively. Curve E is the estimated atmospheric noise level for the Imperial Beach site.

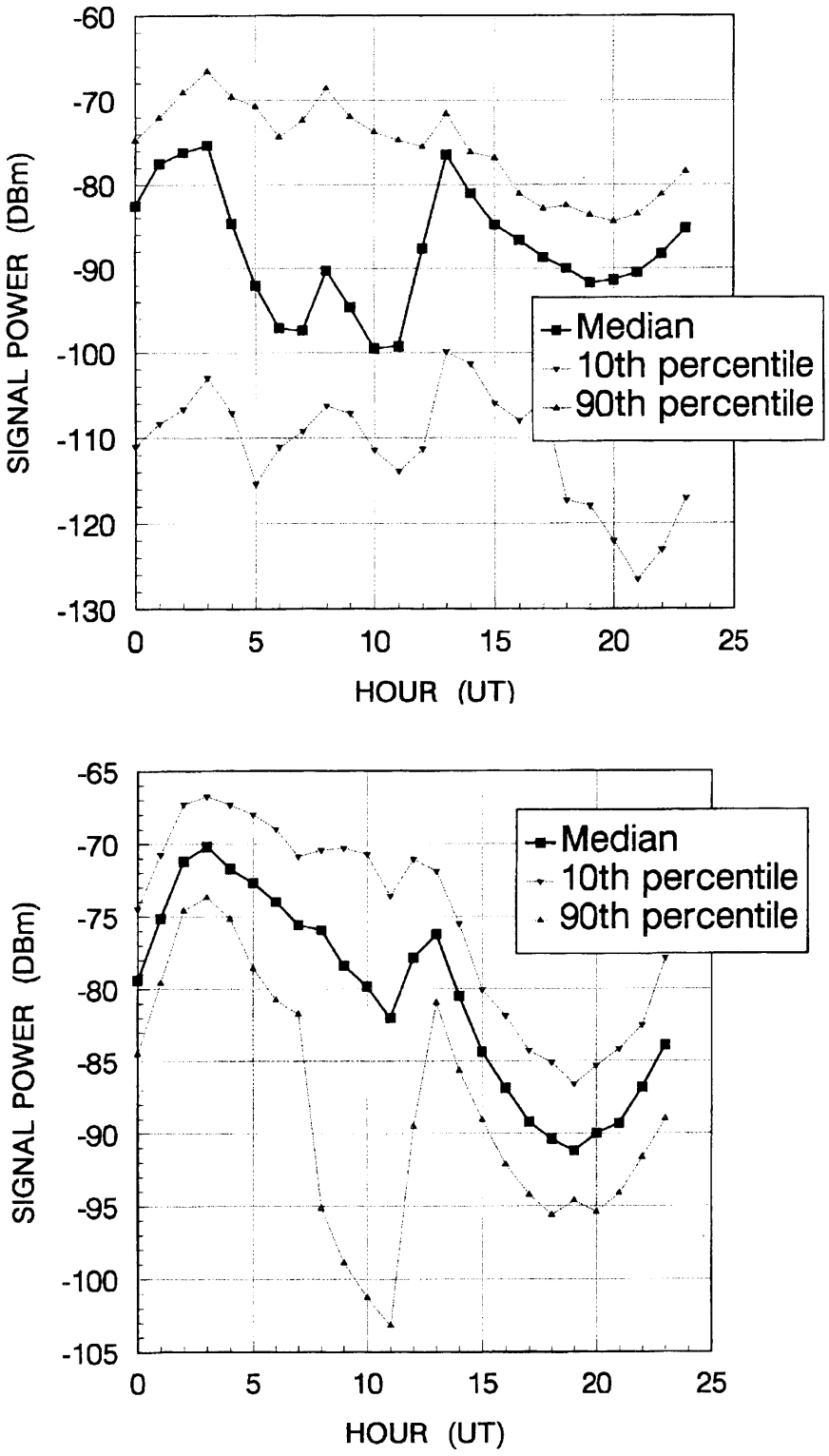

95088005/1

Figure 5. Signal power at 7.8 MHz for April (top) and May (bottom) 1994. Median, 10th percentile, and 90th percentile of the hourly monthly median distribution are shown in separate curves.

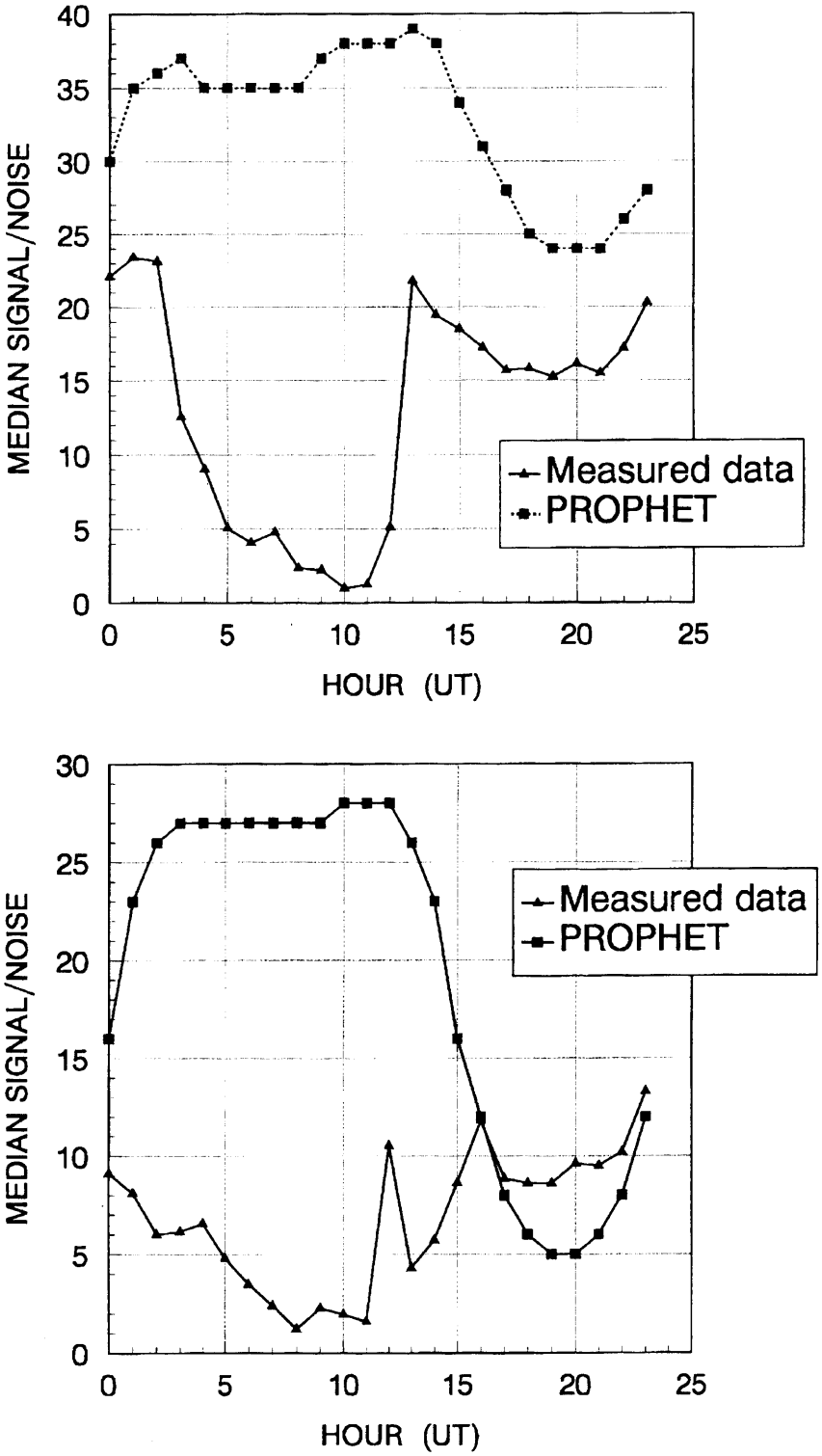

95088006/1

Figure 6. Median signal-to-noise ratio at 7.8 MHz for April (top) and May (bottom) 1994. Also shown are PROPHET predictions for the same period.

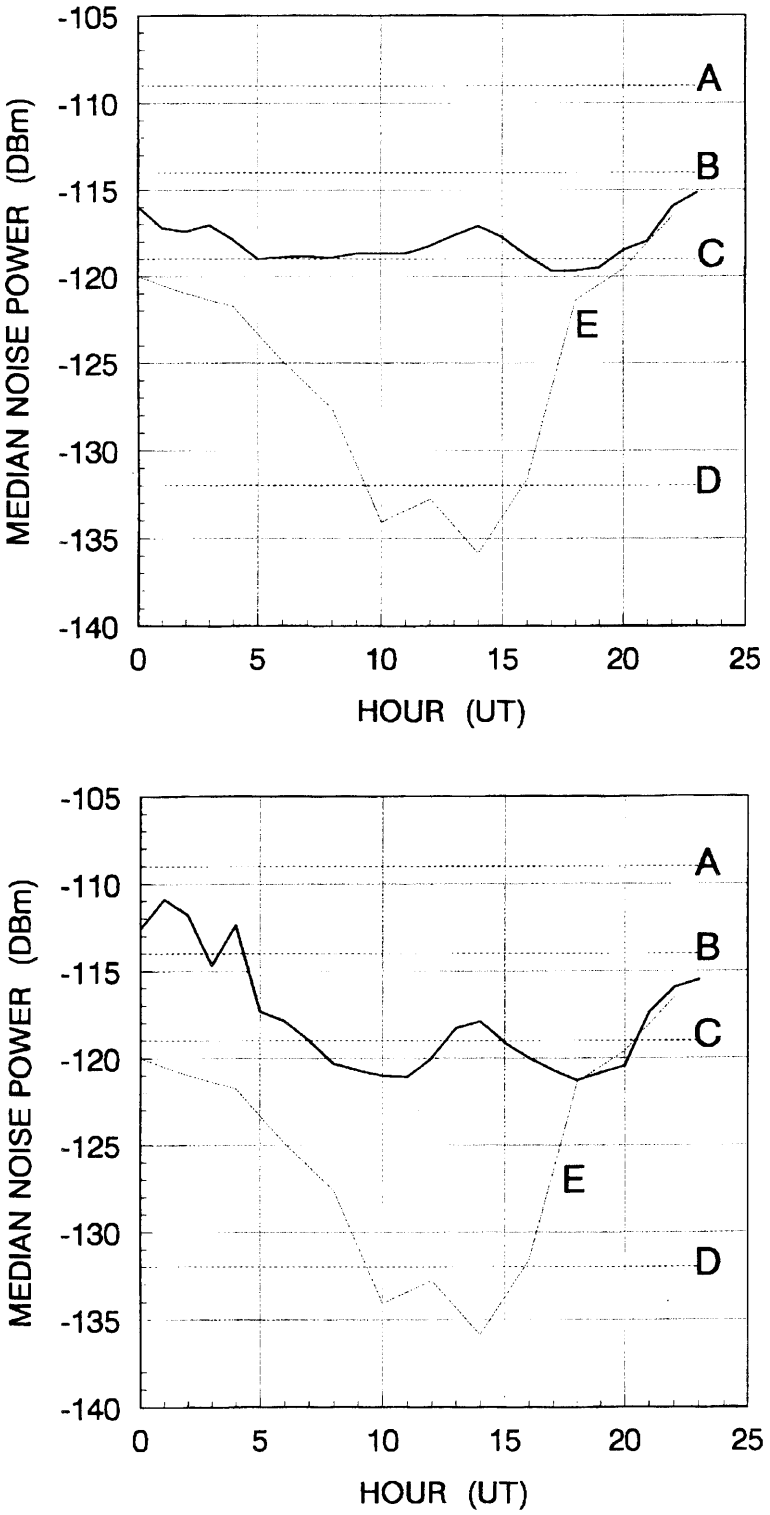

95088007/1

Figure 7. Median noise at 14.4 MHz for April (top) and May (bottom) 1994. Curves A through D are man-made noise estimates for business, residential, rural, and quiet rural, respectively. Curve E is the estimated atmospheric noise level for the Imperial Beach site.

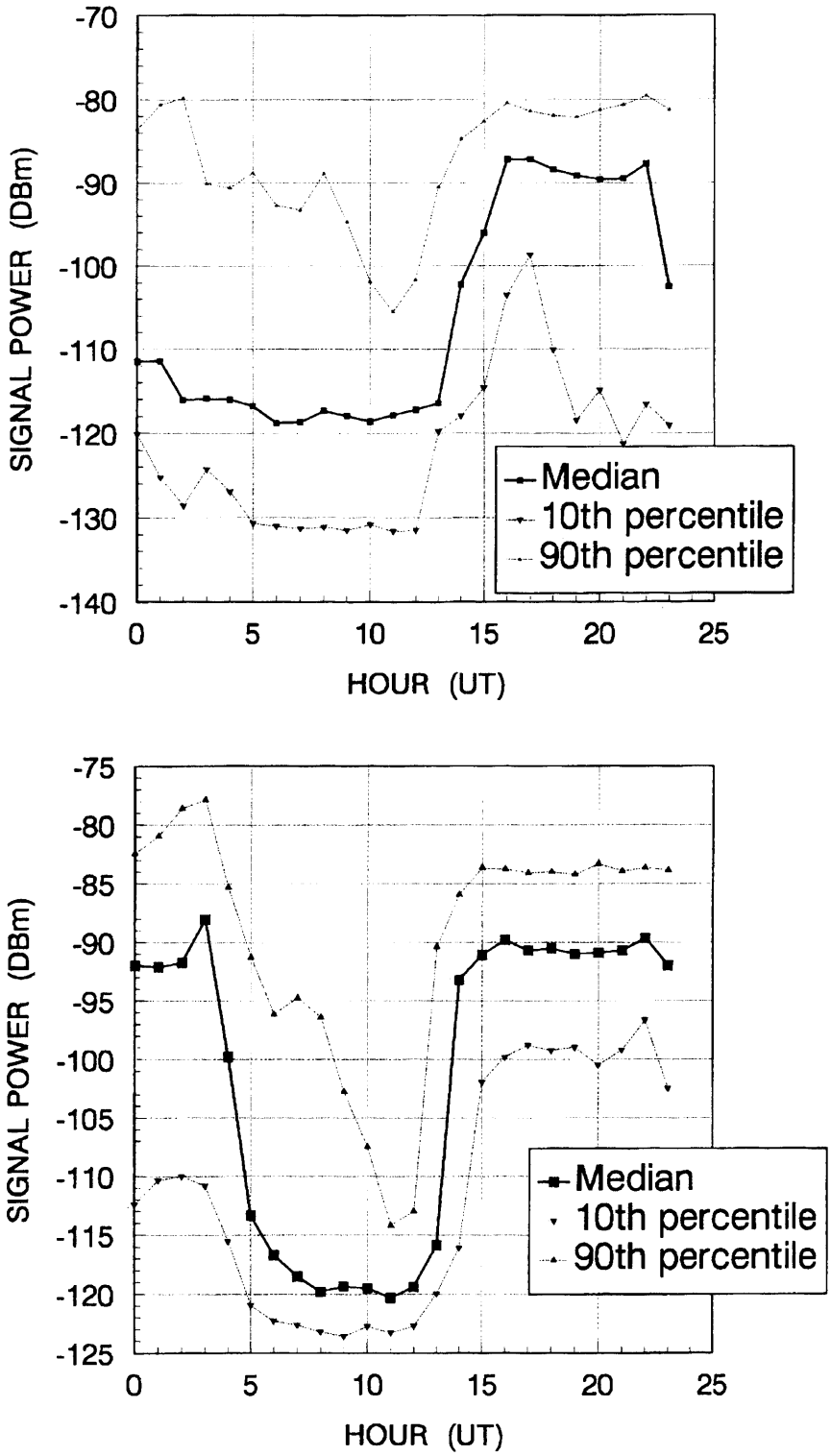

95088008/1

Figure 8. Signal power at 14.4 MHz for April (top) and May (bottom) 1994. Median, 10th percentile, and 90th percentile of the hourly monthly median distribution are shown in separate curves.

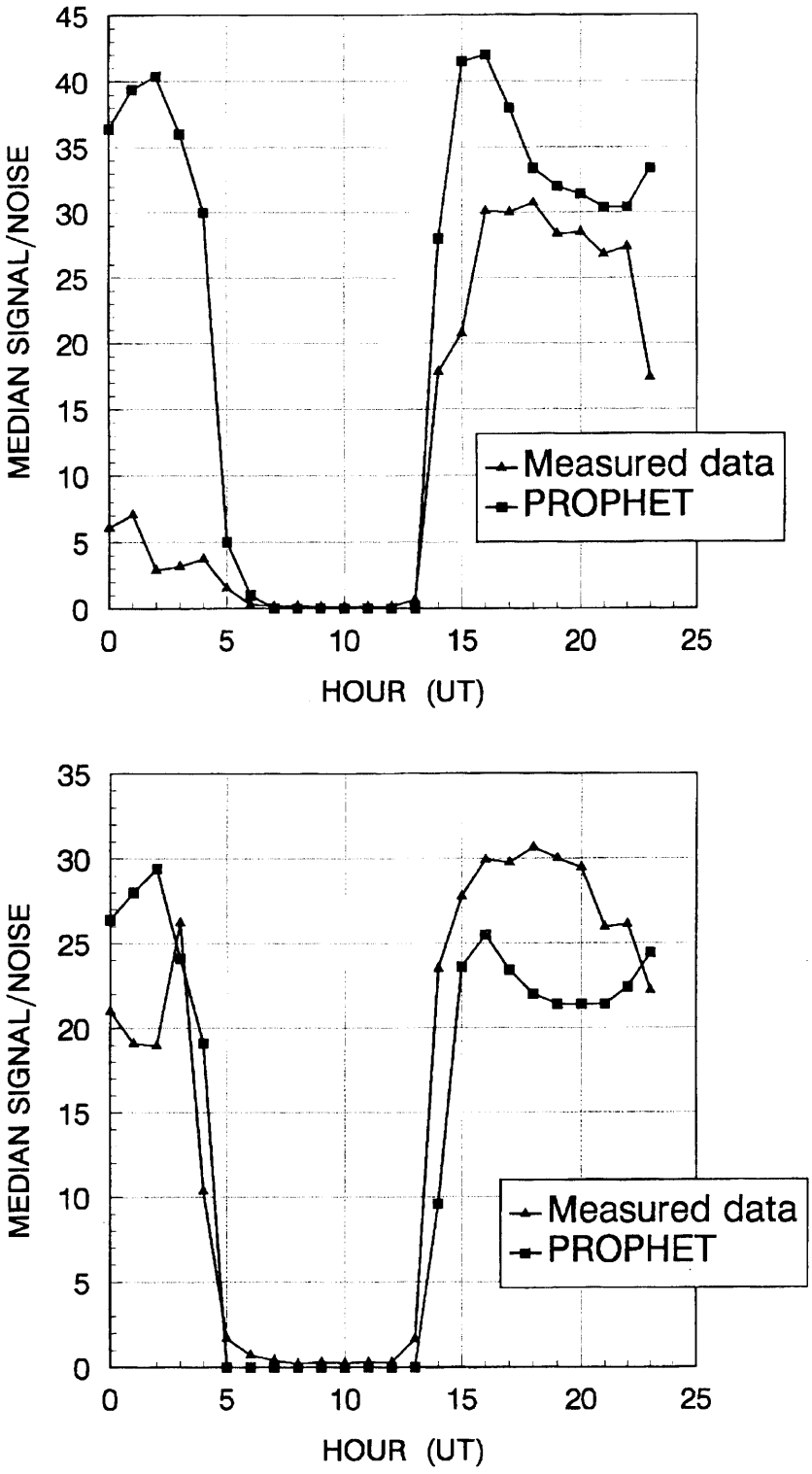

95088009/1

Figure 9. Median signal-to-noise ratio at 14.4 MHz for April (top) and May (bottom) 1994. Also shown are PROPHET predictions for the same period.

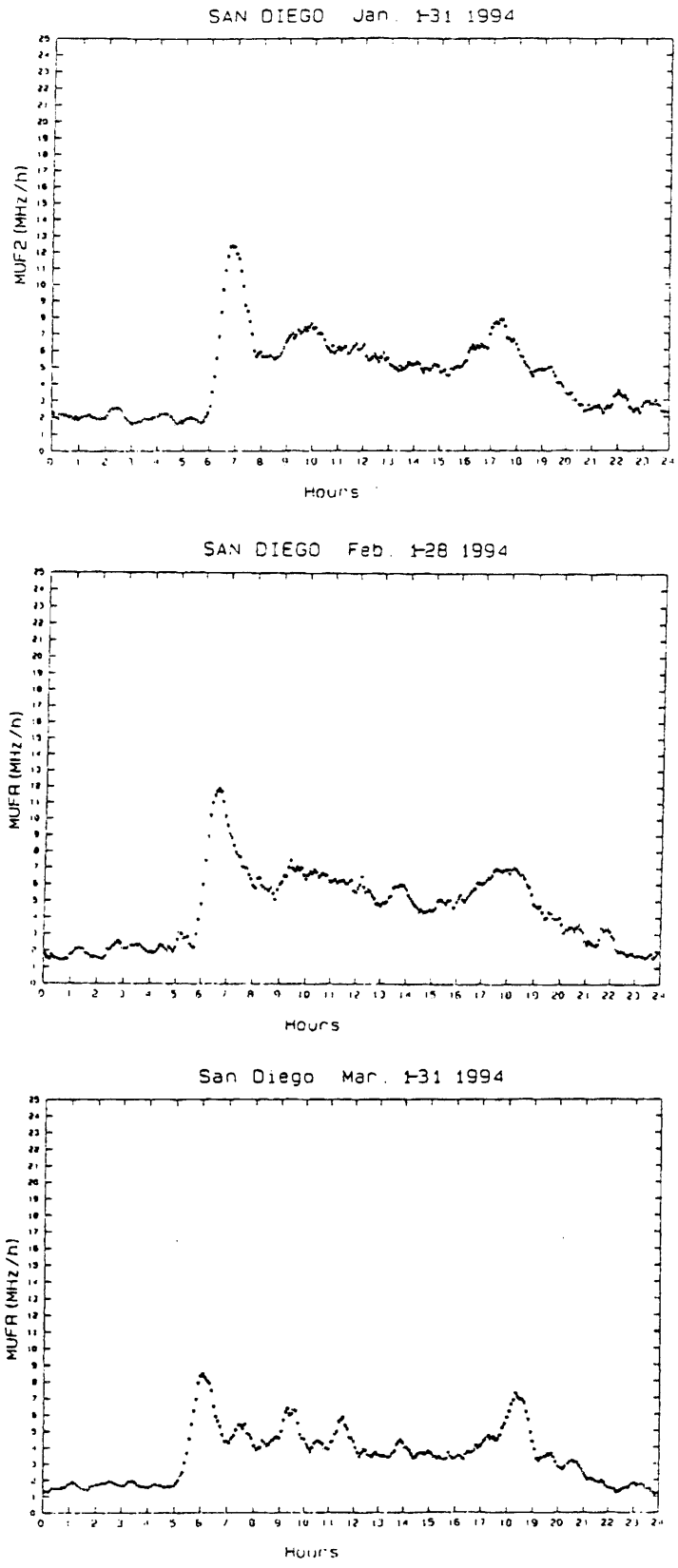

95088010

Figure 10. Variability index for the parameter MUF(3000) for January, February, and March 1994.

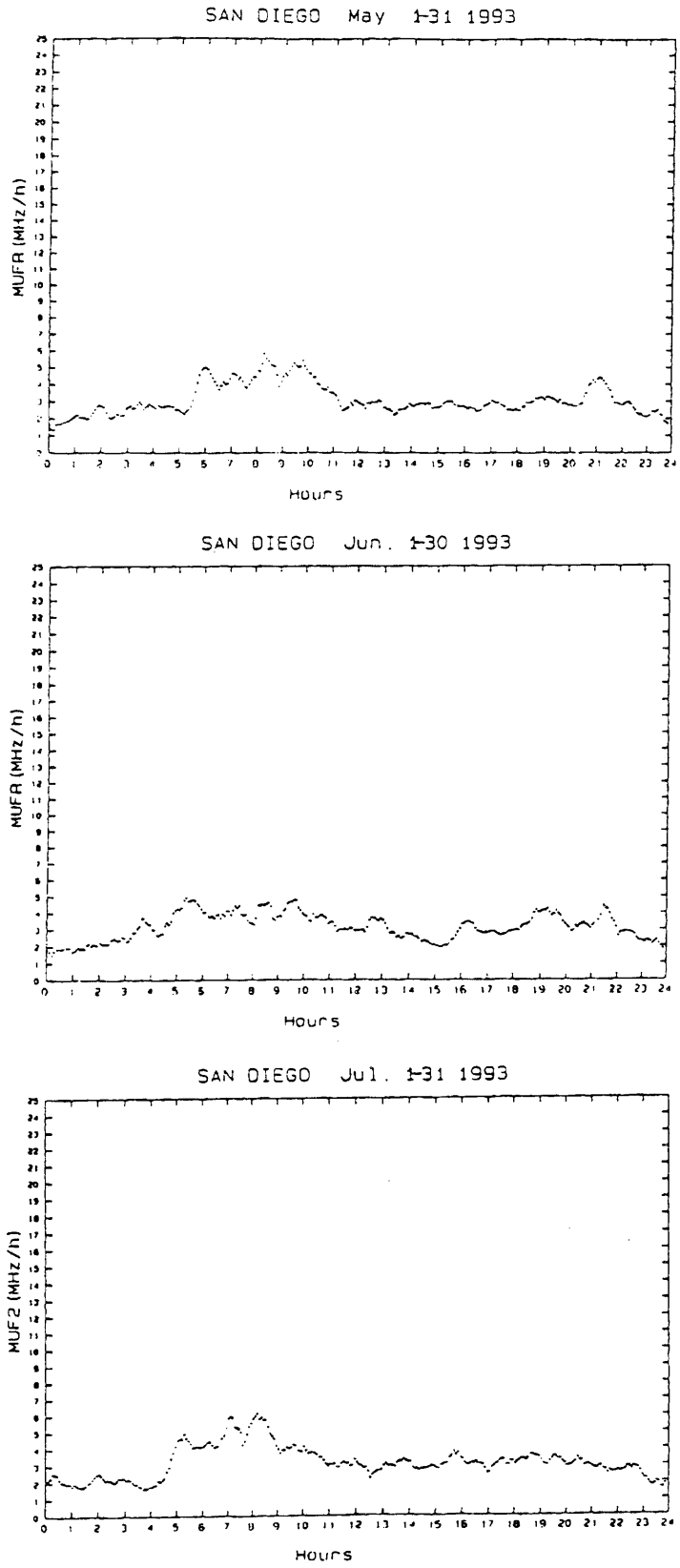

95088011

Figure 11. Variability index for the parameter MUF(3000) for May, June, and July 1993.

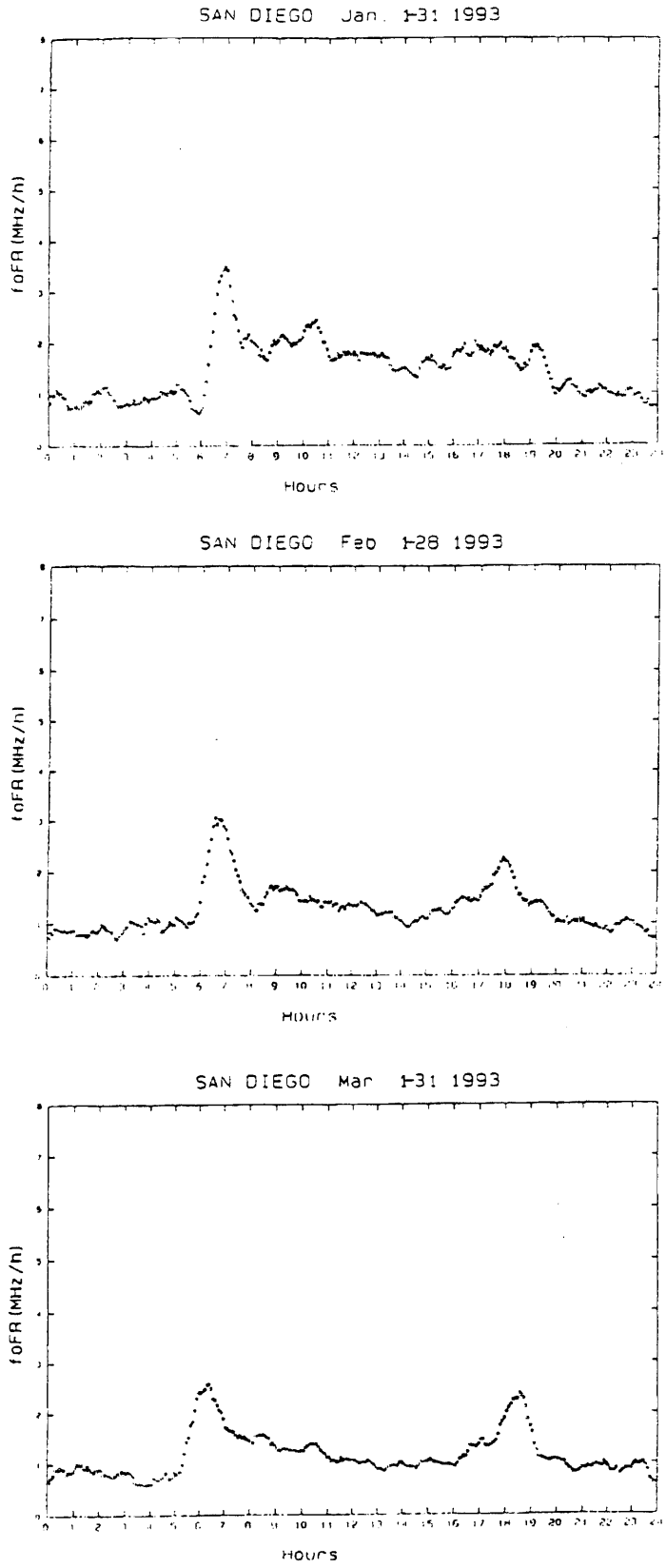

95088012

Figure 12. Variability index for the parameter foF2 for January, February, and March 1993.

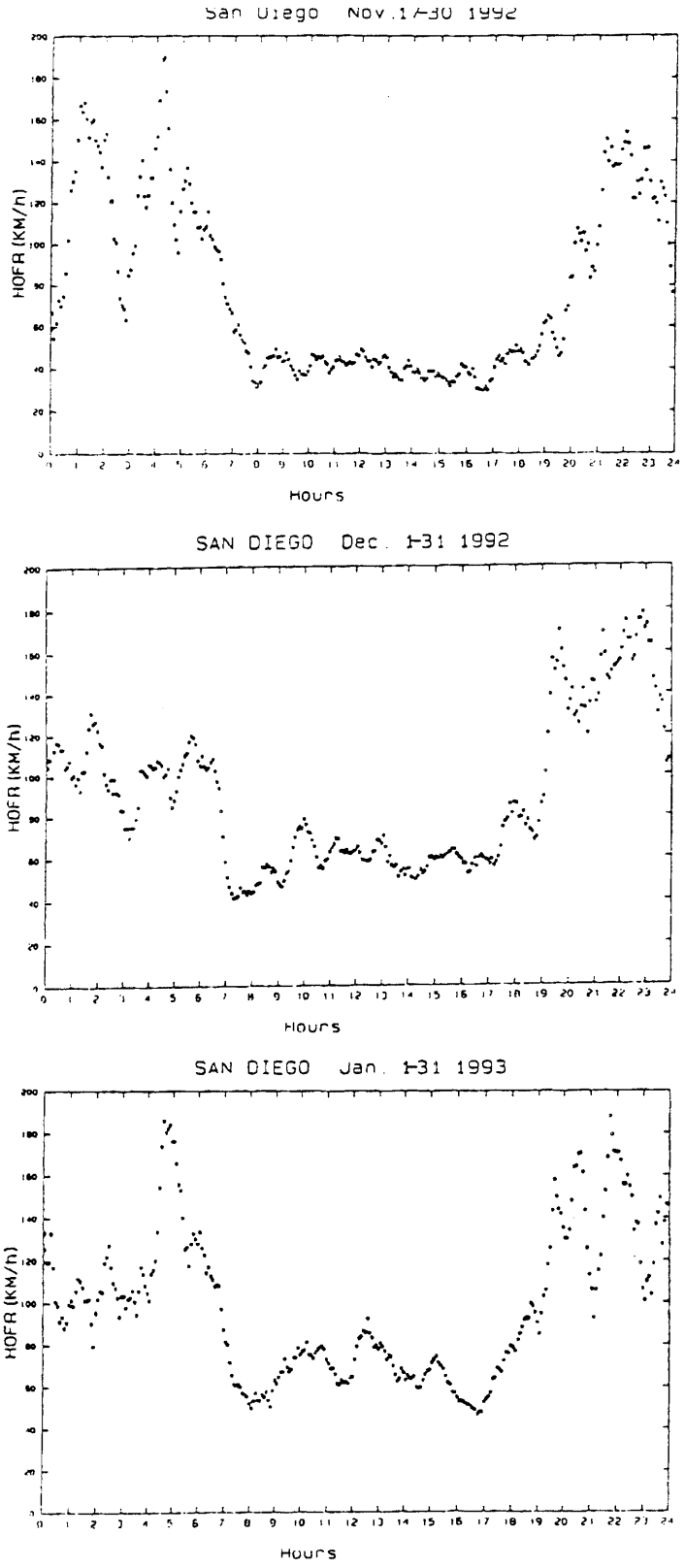

95088013

Figure 13. Variability index for the parameter hmF2 for November and December 1992 and January 1993.

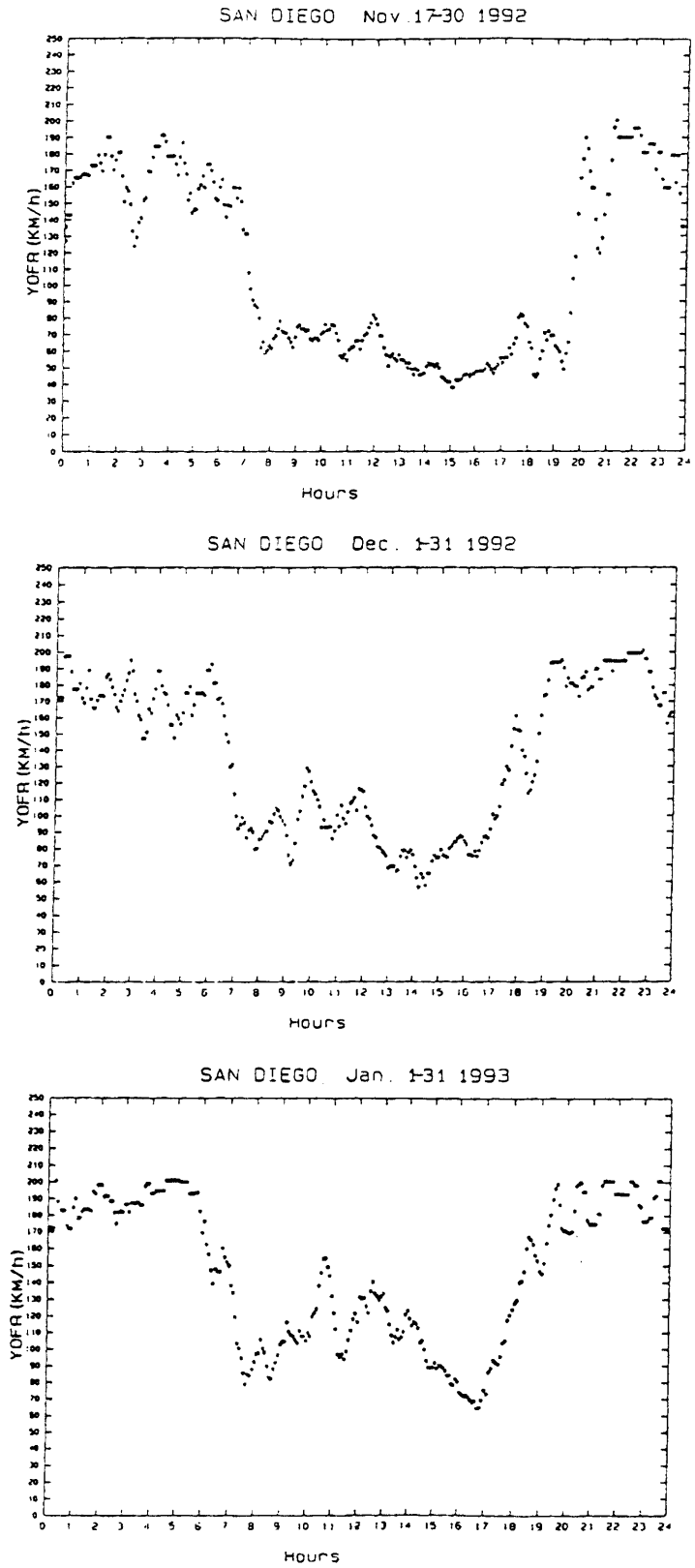

95088014

Figure 14. Variability index for the parameter ymF2 for November and December 1992 and January 1993.

REPORT DOCUMENTATION PAGE

Form Approved
OMB No. 0704-0188

1. AGENCY USE ONLY *(Leave blank)*	2. REPORT DATE	3. REPORT TYPE AND DATES COVERED
	October 1994	Final, FY 94

4. TITLE AND SUBTITLE

MEASUREMENTS OF IONOSPHERIC VARIABILITY

5. FUNDING NUMBERS

0602435N
MPB1
RO35E81
DM302214

6. AUTHOR(S)

R. A. Sprague

7. PERFORMING ORGANIZATION NAME(S) AND ADDRESS(ES)

Naval Command, Control and Ocean Surveillance Center (NCCOSC)
RDT&E Division
San Diego, California 92152−5001

8. PERFORMING ORGANIZATION REPORT NUMBER

TD 2730

9. SPONSORING/MONITORING AGENCY NAME(S) AND ADDRESS(ES)

In-house

10. SPONSORING/MONITORING AGENCY REPORT NUMBER

11. SUPPLEMENTARY NOTES

12a. DISTRIBUTION/AVAILABILITY STATEMENT

Approved for public release; distribution is unlimited.

12b. DISTRIBUTION CODE

13. ABSTRACT *(Maximum 200 words)*

This document reports on FY 94 progress in the ongoing measurement of ionospheric variability. Two measurement campaigns are described and results-to-date are presented. Comparisons of measured signal power are made to predictions from the PROPHET ionnospheric propagation model. Examples of a new variability index for several ionospheric F-region parameters (foF2, MUF(3000), hmF2, and ymF2) are presented.

14. SUBJECT TERMS

electromagnetic propagation atmosphere ionospheric variability

15. NUMBER OF PAGES

16. PRICE CODE

17. SECURITY CLASSIFICATION OF REPORT	18. SECURITY CLASSIFICATION OF THIS PAGE	19. SECURITY CLASSIFICATION OF ABSTRACT	20. LIMITATION OF ABSTRACT
UNCLASSIFIED	UNCLASSIFIED	UNCLASSIFIED	SAME AS REPORT